



Original Article

# One-step Synthesis of Molybdenum Oxide/graphene Composites

Minh Nhat Dang<sup>1,\*</sup>, Do Nhat Minh<sup>2</sup>, Le Ngoc Trung<sup>2</sup>, Nguyen Thanh Hai<sup>2</sup>,  
Le Trong Lu<sup>3,4</sup>, Le Thi Thanh Tam<sup>4</sup>, Nguyen Tuan Hong<sup>2</sup>, Nguyen Van Thao<sup>2</sup>,  
Phan Ngoc Minh<sup>2,3</sup>, Phan Ngoc Hong<sup>2,3,\*</sup>

<sup>1</sup>*Australian Research Council (ARC) Industrial Transformation Training Centre in Surface Engineering for Advanced Materials (SEAM), Faculty of Science, Engineering and Technology, Swinburne University of Technology, PO Box 218, Hawthorn, VIC 3122, Australia*

<sup>2</sup>*Centre for High Technology Development, Vietnam Academy of Science and Technology (VAST), 18 Hoang Quoc Viet, Hanoi, Vietnam.*

<sup>3</sup>*Graduate University of Science and Technology, VAST, 18 Hoang Quoc Viet, Hanoi, Vietnam.*

<sup>4</sup>*Institute for Tropical Technology, VAST, 18 Hoang Quoc Viet, Hanoi, Vietnam.*

Received 09 May 2020

Revised 07 June 2020; Accepted 23 July 2020

**Abstract:** We herein introduce a new approach to synthesize MoO<sub>2</sub>/graphene composites via plasma-enhanced electrochemical exfoliation process. Our samples were prepared by electrifying graphite rods in (NH<sub>4</sub>)<sub>2</sub>Mo<sub>7</sub>O<sub>24</sub> solution under a DC voltage of 70V. By controlling the experimental parameters such as the initial ratio of [Mo<sub>7</sub>O<sub>24</sub>]<sup>2-</sup> precursor, the current and time, we can modify the size and the size distribution of MoO<sub>2</sub> nanoparticles on graphene sheets. The composites were characterized with Scanning Electron Microscopy, Transmission Electron Microscopy, X-ray Diffraction and Raman Spectroscopy.

**Keywords:** graphene, plasma, electrochemistry, MoO<sub>2</sub>, molybdenum oxide, composite

## 1. Introduction

As global warming has turned into a significant environmental challenge due to the overwhelming consumption of fossil-fuel, energy conversion and storage devices play a crucial role in our modern society. To overcome this obstacle, diverge energy storage and conversion systems have been created

\*Corresponding author.

Email address: [nhatminh@swin.edu.au](mailto:nhatminh@swin.edu.au) and [hongpn@htd.vast.vn](mailto:hongpn@htd.vast.vn)

<https://doi.org/10.25073/2588-1124/vnumap.4521>

based on several criteria: low-cost, environmental-friendly behaviour and effectiveness. Lithium-ion batteries (LIBs) are considered one of the most practical and useful devices developed for energy storage [1]. Being emerged only since the early of the 1990s, LIBs have received much interest from scientists in the field of fundamental study and applied research because of its superior properties such as large capacity, high power/energy density, long cycle life and low toxicity [2]. In recent years, one of the challenges to chemists and materials scientists has been developing new electrode materials to improve energy density and reducing cost while maintaining a high rate performance of LIBs. For this reason, various transition-metal oxide nanoparticles (NPs) have attracted considerable attention as the type of ideal electrode materials owing to their high theoretical electrochemical capacities such as  $\text{Fe}_3\text{O}_4$ ,  $\text{Co}_3\text{O}_4$ ,  $\text{MoO}_3$ ,  $\text{V}_2\text{O}_5$  and  $\text{TiO}_2$  [3]. Among them, molybdenum oxide ( $\text{MoO}_2$ ) is considered as a promising candidate to make anode material due to its high capacitances ( $838 \text{ mAhg}^{-1}$ ), low electrical resistivity, high density, high melting point, and excellent chemical stability [4]. However, bulk  $\text{MoO}_2$  undergoes significant volume change by lithium insertion/extraction resulting in poor cycling stability [4–6].

Graphene – a distinct two-dimensional material is also a potential material for use in LIBs. Aside from carbon nanotubes [7,8], they exhibit unique properties such as high electrical conductivity, the large surface area of more than  $2600 \text{ m}^2/\text{g}$  and chemical stability [9,10]. Notably, the excellent electron mobility of  $\text{sp}^2$ -carbon matrix in graphene is expected to enhance overall electrical conductivity. Recent reports have indicated that the formation of graphene/metal oxide composites possibly inherits synergistic effects of the two components, yielding outstanding electrochemical performances. Multi-layer graphene sheets are used as a conductive substrate for metal oxide nanoparticles decorated on their surface. They, furthermore, also hinder metal oxide nanoparticles from the volume changes and aggregation during charge/discharge processes. In contrast, the attachment of metal oxide on graphene effectively inhibits the restacking mechanism of graphene layers [11].

There have been various proposed methods to synthesize  $\text{MoO}_2$ /graphene nanocomposites for a decade. Most methods require a two-step time-consuming mechanism: the oxidation of graphite with the reduction of graphite oxide and the hybridized precursor in extreme condition. The development of facile and easily scaled up synthetic methods, thus, is highly desired. In this study, our group aims to develop a one-step and straightforward approach: plasma-enhanced electrochemical exfoliation process ( $\text{PE}^3\text{P}$ ). The method is based on the generation of a high electric field by applying a voltage of 70 V on a minimal contact area between the tip of the cathode and the electrolyte [12]. This high energy instantly breaks through the air-gap insulator then creates the plasma at cathode tip. Plasma-assisted exfoliation method was first used for the exfoliation of graphene sheets from graphite rod, and by modifying the electrolyte, different types of graphene-based composites can be formed [13,14]. This  $\text{PE}^3\text{P}$  is facile, one-step, low-cost, environmentally friendly in the synthesis of both graphene sheets and  $\text{MoO}_2$  nanoparticles.

## 2. Experimental Setup

### 2.1. Chemicals

Ammonium molybdate ( $(\text{NH}_4)_6\text{Mo}_7\text{O}_{24}\cdot 4\text{H}_2\text{O}$ ),  $\text{H}_2\text{SO}_4$ , KOH, cylindrical high purity graphite rod (5 mm, 30 mm in length with 99.99%) were ordered from Sigma-Aldrich. A Pt plate (10 x 25 x 0.3 mm, 99.99%) plays a role of anode electrode. No further purification is required.

### 2.2. Synthesis of $\text{MoO}_2$ /graphene

$\text{MoO}_2$ /graphene composite was synthesized by plasma-enhanced electrochemical exfoliation method according to the following procedure: 1.5 mol  $(\text{NH}_4)_6\text{Mo}_7\text{O}_{24}\cdot 4\text{H}_2\text{O}$  were adding to 150 mL  $\text{H}_2\text{SO}_4$  solution (with a concentration of 0.5 M, 1 M, 3 M, respectively) as the electrolyte. Graphite and

Pt electrodes were used as cathode and anode, respectively. Cathodic graphite tip was sharpened to 1 mm in diameter and immersed approximately 1 mm into the solution, while the Pt electrode was submerged deeply into the solution. Then, a constant voltage of 70 V from a DC source (110V-3A, Kikusui Electronic corp., Japan) was applied between two electrodes, and current intensity was controlled in the range from 0.4 to 0.6 A. The reaction lasted for one hour within an ultrasonication bath at ambient condition. For every 15 minutes, the graphite electrode requires a re-sharpening process to ensure the sharpened tip. The obtained suspension was filtered and washed carefully with distilled water and ethanol by vacuum filtration system with a polyvinylidene fluoride membrane (pore size of 0.2  $\mu\text{m}$ ) until reaching to neutral  $\text{pH} = 7$ . Then, after being dried at  $60^\circ\text{C}$  for one hour, the final products were collected. A similar process was applied with different concentration of precursors. Samples GMo1, GMo5 and GMo10 are denoted respectively for the initial concentration of ammonium molybdate as 1 mM, 5 mM and 10 mM.

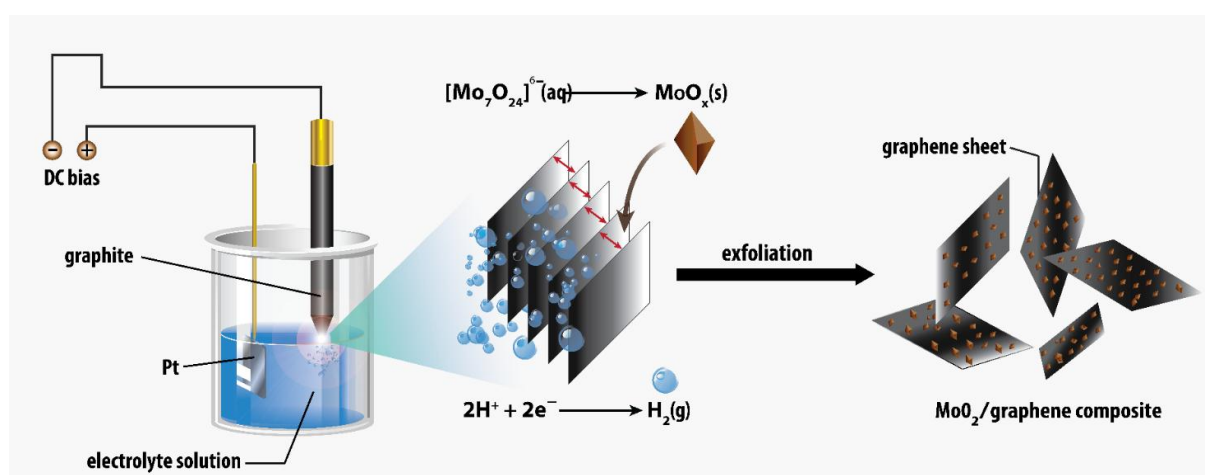


Figure 1. Schematic setup of the synthesis of  $\text{MoO}_2/\text{graphene}$  composites.

### 2.3. Characterization Preparation

Scanning electron microscopy (SEM) images were recorded on a Hitachi S-4800 Field Emission SEM. SEM samples were prepared by drop-drying from a water/ethanol suspension of the composite material on a Si wafer. Transmission electron microscopy (TEM – Hitachi 9500, 300 kV) were conducted using specimens dispersed in ethanol and then dropped onto copper microgrid coated with a holey carbon film, followed by the evaporation of the ethanol.

The crystallographic structure of the samples was determined by a D2 XRD system (Equinox 5000) equipped with a  $\text{Cu K}\alpha$  radiation and a Ni filter ( $\lambda = 0.1542 \text{ nm}$ ).

A LabRam HR Evolution recorded Raman spectra with a laser wavelength of 532nm.

## 3. Results and Discussion

Surface morphology of the molybdenum oxide/graphene composites was characterized by using SEM. Figure 2 shows the SEM images of the samples prepared at different initial concentrations of  $[\text{Mo}_7\text{O}_{24}]^{6-}$ . As can be seen, spherical  $\text{MoO}_x$  nanoparticles were decorated on the surface of layer-by-

layer graphene sheets, exhibiting the successful formation of  $\text{MoO}_x/\text{graphene}$  composites. The diameter of the  $\text{MoO}_x$  nanoparticles was likely under 30 nm. When the concentration increases, oxide particles decrease in size and attain wider distribution on the surface of graphene sheets. In the TEM images, graphene is observed with under 10 layers (Figure 3a). Manganese oxides appear in the nanoclusters form as in Figure 3b.

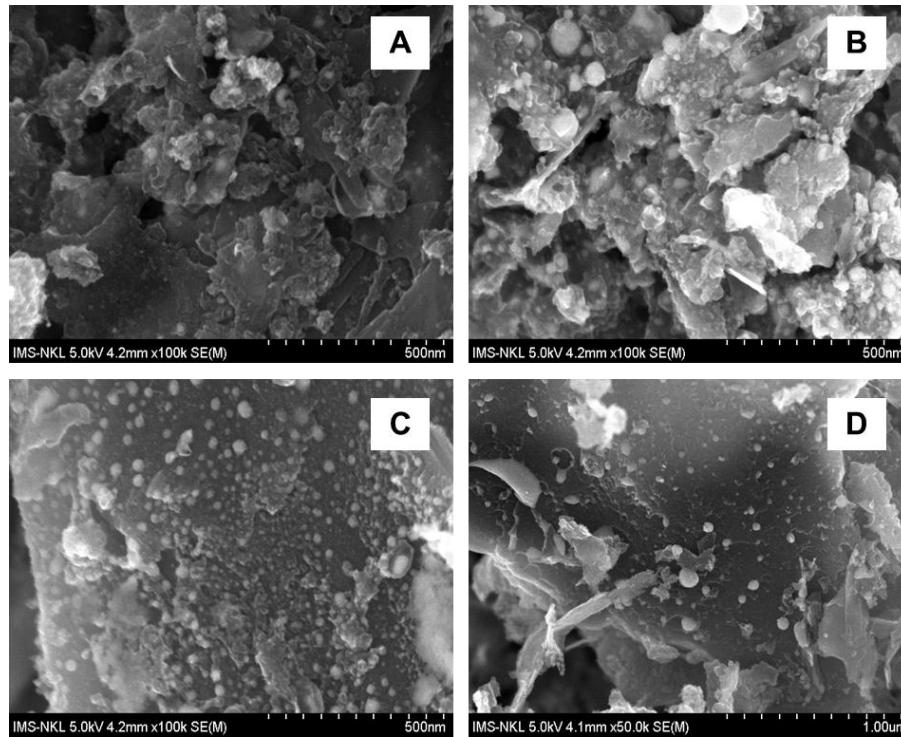


Figure 2. SEM images of  $\text{MoO}_x/\text{graphene}$  composite at different precursor concentrations: A) GMo1, B) GMo5 and C-D) GMo10.

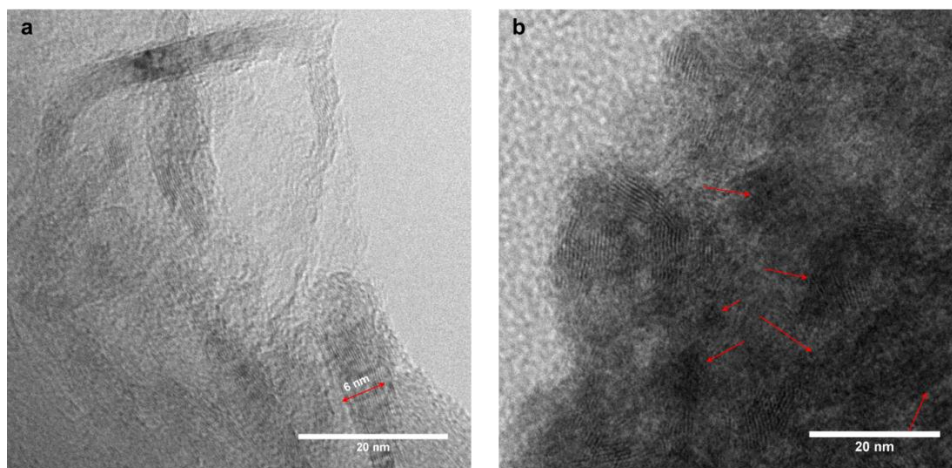


Figure 3. TEM images of (a) Graphene and (b) GMo1 with red arrows pointing at nanoclusters.

X-ray diffraction was performed to identify the composition of the as-prepared  $\text{MoO}_x/\text{graphene}$  composite (Figure 4). It can be observed that the diffraction peaks at  $2\theta$  values of  $26.65^\circ$ ,  $36.65^\circ$ ,  $53.7^\circ$  and  $61.35^\circ$  corresponding to the (110), (020), (220) and (031) planes of monoclinic crystal phases of  $\text{MoO}_2$  (JCPDS No. 65 – 5787) [15]. No characteristic peak is observed for impurities such as  $\text{MoO}_3$  as well as other molybdenum oxides, indicating the direct reduction of  $\text{Mo}^{\text{VI}}$  to  $\text{Mo}^{\text{IV}}$  during the electrochemical process. Thus, molybdenum oxide  $\text{MoO}_x$  in this work is evidently proved as  $\text{MoO}_2$ . Additionally, the presence of two diffraction peaks at  $2\theta$  of  $26.65^\circ$  and  $42.45^\circ$  is assigned to the (002) and (100) basal planes of graphite, respectively (Figure 4a). Also, the intensity of all diffraction peaks is strong and narrow, demonstrating the high crystallinity of the as-synthesized  $\text{MoO}_2/\text{graphene}$  composites.

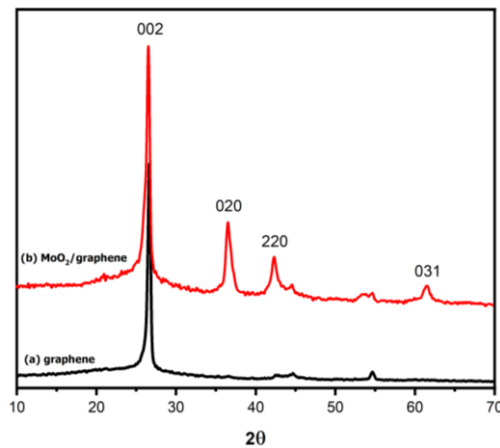


Figure 4. XRD pattern of (a) graphene and (b)  $\text{MoO}_2/\text{graphene}$  composite.

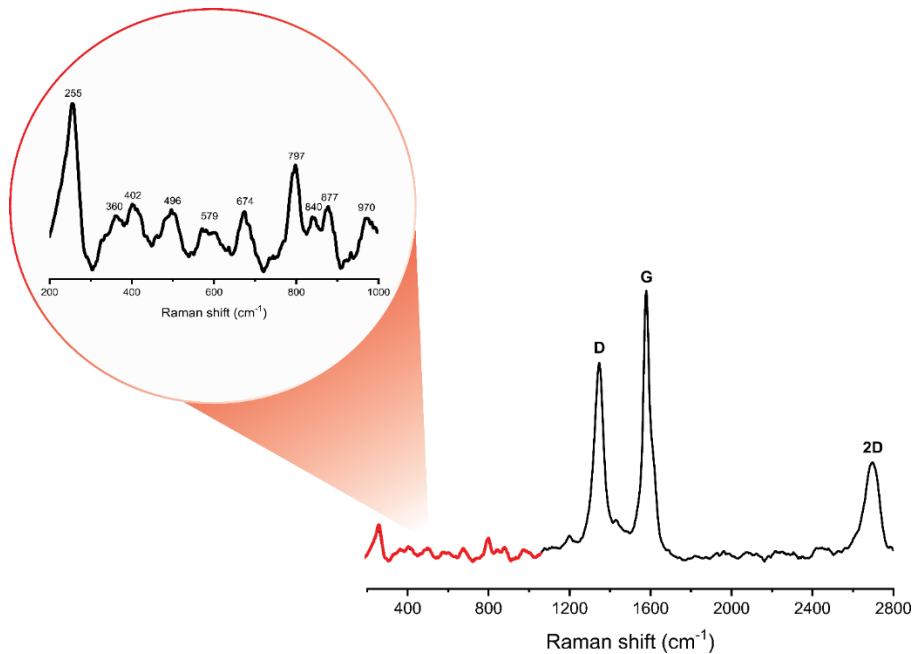


Figure 5. Raman spectrum of  $\text{MoO}_2/\text{graphene}$ .

To further investigate the chemical configuration, the MoO<sub>2</sub>/graphene composites were characterized by Raman spectroscopy (Figure 5). The peaks at 1344, 1578 and 2696 cm<sup>-1</sup> are attributed to D, G and 2D bands of graphene sheets, respectively. The G band represents the in-plane vibration of sp<sup>2</sup> carbon atoms while the D band stands for defect structure of graphene. Thus, high-intensity peak corresponds to edges region, where the central area of the graphene sheet rarely exhibits D bands [16,17]. The high intensity of the D band is observed, indicating the significant content of defects in the graphene sheets (Figure 4a). The formation of new edges caused it during the exfoliation of graphite and MoO<sub>2</sub> nanoparticles generated onto the surface of graphene sheets. The 2D band, so-called the second-order of zone boundary phonons [17], shows a signature Raman spectrum for most sp<sup>2</sup> material. The broaden 2D band indicates that the graphene has a multi-layer structure.

Furthermore, in the range of below 1000 cm<sup>-1</sup>, the characteristic peaks of MoO<sub>2</sub> mostly shifted to the left. Raman peaks at 970, 797, 674 cm<sup>-1</sup> are seemingly originated from position 993, 820 and 663 cm<sup>-1</sup>, corresponding to Mo = O bond stretching (A<sub>g</sub>, ν<sub>as</sub>), Mo = O bond stretching (A<sub>g</sub>, ν<sub>s</sub>) and O – Mo – O bond stretching (B<sub>2g</sub>, B<sub>3g</sub>, ν<sub>a</sub>) [18].

#### 4. Conclusion

In summary, MoO<sub>2</sub>/graphene composites were successfully synthesized via a one-step method with low-cost equipment and simple setup at ambient. The results reveal that MoO<sub>2</sub> nanoparticles sized under 30nm were decorated randomly on the surface of multi-layer graphene sheets. With the potential of being scaled up, PE<sup>3</sup>P process could be optimized and developed for the preparation of other graphene-based materials.

#### Acknowledgments

The authors acknowledge the financial support from National Foundation for Science and Technology Development (NAFOSTED Grant No. 103.99-2017.360) and Vietnam Academy of Science and Technology (Grant No. NVCC42.01/20-20). Parts of this research was conducted by the Australian Research Council (ARC) Industrial Transformation Training Centre in Surface Engineering for Advanced Materials (SEAM), via Award number IC180100005, Swinburne University of Technology, Hawthorn, Victoria 3122, Australia.

#### References

- [1] C. Zhang, P. Zhang, J. Dai, H. Zhang, A. Xie, Y. Shen, Facile synthesis and electrochemical properties of MoO<sub>2</sub>/reduced graphene oxide hybrid for efficient anode of lithium-ion battery, *Ceram. Int.* 42 (2016) 3618–3624. <https://doi.org/10.1016/j.ceramint.2015.11.026>.
- [2] A.S. Aricò, P. Bruce, B. Scrosati, J.-M. Tarascon, W. van Schalkwijk, Nanostructured materials for advanced energy conversion and storage devices, *Nat. Mater.* 4 (2005) 366–377. <https://doi.org/10.1038/nmat1368>.
- [3] A. Yu, H.W. Park, A. Davies, D.C. Higgins, Z. Chen, X. Xiao, Free-Standing Layer-By-Layer Hybrid Thin Film of Graphene-MnO<sub>2</sub> Nanotube as Anode for Lithium Ion Batteries, *J. Phys. Chem. Lett.* 2 (2011) 1855–1860. <https://doi.org/10.1021/jz200836h>.
- [4] J.-P. Jégou, H.-K. Kim, J.-S. Kim, K.-B. Kim, One-pot synthesis of mixed-valence MoO<sub>x</sub> on carbon nanotube as an anode material for lithium ion batteries, *J. Electroceramics.* 31 (2013) 218–223. <https://doi.org/10.1007/s10832-013-9821-0>.

- [5] Y.S. Jung, S. Lee, D. Ahn, A.C. Dillon, S.-H. Lee, Electrochemical reactivity of ball-milled  $\text{MoO}_3$ -y as anode materials for lithium-ion batteries, *J. Power Sources*. 188 (2009) 286–291. <https://doi.org/10.1016/j.jpowsour.2008.11.125>.
- [6] J. Cabana, L. Monconduit, D. Larcher, M.R. Palacín, Beyond Intercalation-Based Li-Ion Batteries: The State of the Art and Challenges of Electrode Materials Reacting Through Conversion Reactions, *Adv. Mater.* 22 (2010) E170–E192. <https://doi.org/10.1002/adma.201000717>.
- [7] N. Thanh Hai, D. Nhat Minh, D. Nhat Minh, N. Dinh Dung, L. Nhu Hai, P. Ngoc Hong, N. Tuan Hong, Hot-filament CVD Growth of Vertically-aligned Carbon Nanotubes on Support Materials for Field Electron Emitters, *VNU J. Sci. Math. - Phys.* 36 (2020) 98–105. <https://doi.org/10.25073/2588-1124/vnumap.4477>.
- [8] M.N. Dang, M.D. Nguyen, N.K. Hiep, P.N. Hong, I.H. Baek, N.T. Hong, Improved field emission properties of carbon nanostructures by laser surface engineering, *Nanomaterials*. 10 (2020). <https://doi.org/10.3390/nano10101931>.
- [9] E. Yoo, J. Kim, E. Hosono, H. Zhou, T. Kudo, I. Honma, Large Reversible Li Storage of Graphene Nanosheet Families for Use in Rechargeable Lithium Ion Batteries, *Nano Lett.* 8 (2008) 2277–2282. <https://doi.org/10.1021/nl800957b>.
- [10] Z.-S. Wu, G. Zhou, L.-C. Yin, W. Ren, F. Li, H.-M. Cheng, Graphene/metal oxide composite electrode materials for energy storage, *Nano Energy*. 1 (2012) 107–131. <https://doi.org/10.1016/j.nanoen.2011.11.001>.
- [11] G.H. Jeong, S. Baek, S. Lee, S.W. Kim, Metal Oxide/Graphene Composites for Supercapacitive Electrode Materials, *Chem. - An Asian J.* 11 (2016) 949–964. <https://doi.org/10.1002/asia.201501072>.
- [12] M.N. Dang, T.D.T. Ung, H.N. Phan, Q.D. Truong, T.H. Bui, M.N. Phan, L.Q. Nguyen, P.D. Tran, A novel method for preparation of molybdenum disulfide/graphene composite, *Mater. Lett.* 194 (2017) 145–148. <https://doi.org/10.1016/j.matlet.2017.02.018>.
- [13] M.N. Dang, T.H. Nguyen, T. Van Nguyen, T.V. Thu, H. Le, M. Akabori, N. Ito, H.Y. Nguyen, T.L. Le, T.H. Nguyen, V.T. Nguyen, N.H. Phan, One-pot synthesis of manganese oxide/graphene composites via a plasma-enhanced electrochemical exfoliation process for supercapacitors, *Nanotechnology*. 31 (2020) 345401. <https://doi.org/10.1088/1361-6528/ab8fe5>.
- [14] D.N. Minh, H.P. Duong, L. Hoang, P.D. Nguyen, P.D. Tran, P.N. Hong, Plasma-Assisted Preparation of  $\text{MoS}_2$ /Graphene/MOF Hybrid Materials and Their Electrochemical Behaviours, *Mater. Trans.* 61 (2020) 1535–1539. <https://doi.org/10.2320/matertrans.MT-MN2019003>.
- [15] S.-S. Chen, X. Qin, Molybdenum oxide-iron oxide/graphene composite as anode materials for lithium ion batteries, *J. Solid State Electrochem.* 19 (2015) 1867–1874. <https://doi.org/10.1007/s10008-015-2846-3>.
- [16] K. Sasaki, Y. Tokura, T. Sogawa, The Origin of Raman D Band: Bonding and Antibonding Orbitals in Graphene, *Crystals*. 3 (2013) 120–140. <https://doi.org/10.3390/cryst3010120>.
- [17] A.C. Ferrari, J.C. Meyer, V. Scardaci, C. Casiraghi, M. Lazzeri, F. Mauri, S. Piscanec, D. Jiang, K.S. Novoselov, S. Roth, A.K. Geim, Raman Spectrum of Graphene and Graphene Layers, *Phys. Rev. Lett.* 97 (2006) 187401. <https://doi.org/10.1103/PhysRevLett.97.187401>.
- [18] K. Shomalian, M.-M. Bagheri-Mohagheghi, M. Ardyanian, Characterization and study of reduction and sulfurization processing in phase transition from molybdenum oxide ( $\text{MoO}_2$ ) to molybdenum disulfide ( $\text{MoS}_2$ ) chalcogenide semiconductor nanoparticles prepared by one-stage chemical reduction method, *Appl. Phys. A*. 123 (2017) 93. <https://doi.org/10.1007/s00339-016-0719-y>.